

²⁴T. R. Koehler, N. S. Gillis, and D. C. Wallace, *Phys. Rev. B* **1**, 4521 (1970).

²⁵W. R. Marquardt and J. Trivisonno, *J. Phys. Chem. Solids* **26**, 273 (1965).

²⁶E. Gorin, *Phys. Z. Sowjetunion* **9**, 238 (1936).

²⁷C. E. Moore, *Atomic Energy Levels as Derived from Analyses of Optical Spectra*, U.S. Natl. Bur. Stand. Circular No. 467 (U.S. GPO, Washington, D.C., 1949).

²⁸M. Rasolt and R. Taylor, *J. Phys. F* **3**, 67 (1973).

PHYSICAL REVIEW B

VOLUME 8, NUMBER 4

15 AUGUST 1973

Band Structure of NiS as Calculated Using a Simplified Linear-Combination-of-Muffin-Tin-Orbitals Method

R. V. Kasowski

Central Research Department, E. I. du Pont de Nemours and Company, Experimental Station, Wilmington, Delaware 19898*

(Received 16 January 1973)

Hexagonal NiS undergoes a first-order metal-to-nonmetal transition as the temperature is lowered below 264 K. NiS appears to be a "normal Pauli-paramagnetic *d*-band metal" above the transition temperature T_t , while below T_t it is antiferromagnetic (moment $\sim 1.7\mu_B$) and either metallic or semimetallic. By use of a simplified (linear-combination-of-muffin-tin-orbitals) method that no longer requires a secular equation to be calculated as a function of energy, the band structure for NiS is calculated. These results indicate that the *S p* bands overlap the bottom of the *d* bands as hypothesized by White and Mott. It appears that this overlap increases with temperature, as a result of lattice vibrations which are included in the calculation through a Debye-Waller factor. We suggest a Mott-Hubbard transition occurs for a critical electron-phonon coupling which may be associated with a critical temperature.

I. INTRODUCTION

NiS is one of the many transition-metal compounds that undergoes a first-order metal-to-nonmetal (M-NM) phase transition as the temperature is lowered.¹ Mott² has ascribed this transition in NiS to a Hubbard gap since neutron-diffraction³ results indicate the moment is $1.55\mu_B$ below the transition temperature T_t of 264 K but is less than $0.5\mu_B$ above T_t . Mott further supports the Hubbard-gap model by the fact that the high-temperature phase appears to be a normal *d*-band metal, $\rho \sim 10^{-4} \Omega \text{ cm}$ and the magnetic susceptibility is temperature independent ($\sim 2.25 \times 10^{-6} \text{ emu/gm}$). More recently, White and Mott⁴ concluded that NiS undergoes a metal-metal transition (low-temperature resistivity $\rho_{LT} \sim 10^{-2} \Omega \text{ cm}$). Koehler⁵ arrives at the same conclusion on the bases of his low-temperature resistivity and susceptibility measurements.

White and Mott⁴ hypothesize that the moments and the Hubbard gap form as a result of the discontinuous lattice expansion that occurs as T is lowered below T_t . (Hexagonal lattice parameters c and a increase by 1% and 0.3%, respectively, without a change in structure.^{6,7}) Our present work implies an alternative explanation since the energy bands of NiS, calculated with the linear-combination-of-muffin-tin-orbitals (LCMTO) method,^{8,9} are more sensitive to an average electron-phonon coupling or Debye-Waller correction¹⁰ to

the potential than to a discontinuous change in lattice parameters. Consequently, the discontinuous lattice expansion that occurs as the temperature is lowered below T_t appears to result from the spontaneous appearance of local moments as a critical electron-phonon coupling is reached.

There are few theoretical studies such as ours of the M-NM transition in transition-metal compounds based on complete energy-band calculations. Energy bands are difficult to calculate since these transition-metal compounds usually form in structures with more than one molecule per unit cell and the potentials contain large non-muffin-tin contributions. As a result, commonly used first-principles calculational techniques are difficult to apply.¹¹ The orthogonalized-plane-wave (OPW) method cannot easily treat the *d* bands, and the Korringa-Kohn-Rostoker (KKR) method cannot treat the non-muffin-tin part of the potential. Augmented-plane-wave (APW) and linear-combination-of-atomic-orbitals (LCAO) methods can treat the non-muffin-tin potential but require a large basis set when there are several atoms per unit cell. The LCMTO method,^{8,9} however, has the advantage of being able to treat the non-muffin-tin potential with a small basis set, thus making it convenient for complex systems such as NiS.

In addition, the LCMTO has the added advantage, not found with KKR and APW, that the secular equation need not be calculated as a function of the energy E , which serves as a nonlinear varia-

tional parameter to obtain the lowest-energy states. In the present paper, we show that the nonlinear variational parameters in LCMTO are only weakly sensitive to the band symmetries, and a single set of parameters is valid for the entire calculation. Consequently, the same basis set is used for all \vec{k} points and the secular equation is now in convenient LCAO form, $\langle |H - E| \rangle$, which is diagonalized only once at each \vec{k} point. This simplified LCMTO approach is discussed in Sec. II.

Section III is concerned with the effects of thermal expansion and thermal lattice vibrations on the potential. The energy bands and the effects of temperature are presented in Sec. IV. Section V discusses how the M-NM transition might occur based on these band calculations.

II. SIMPLIFIED LCMTO

Before describing the simplification involved in computing bands for complex crystals such as NiS, we briefly review the general theoretical framework underlying the LCMTO method. The potential, formed by overlapping atomic charge densities, is expanded in spherical harmonics within nonoverlapping atomic Wigner-Seitz (AWS) cells. Solutions $\phi_{lm}(E, \mathbf{r})$ of the Schrödinger equation for the muffin-tin part of the potential are then used to construct muffin-tin orbitals (MTO's):

$$\chi_{lm}(E, \kappa, \mathbf{r}) = \begin{cases} \phi_{lm}(E, \vec{\mathbf{r}}) + C_l(E, \kappa) \bar{J}_{lm}(\kappa, \vec{\mathbf{r}}), & r \leq S \\ -s_l(E, \kappa) \bar{K}_{lm}(\kappa, \vec{\mathbf{r}}), & r \geq S. \end{cases}$$

C_l and s_l are determined by continuity of the logarithmic derivative at the muffin-tin sphere radius S . $\bar{J}_{lm}(\kappa, \vec{\mathbf{r}})$ is that solution $J_{lm}(\kappa, \vec{\mathbf{r}})$ of the wave equation which is orthogonalized to the core states of the potential at the origin, while $\bar{K}_{lm}(\kappa, \vec{\mathbf{r}})$ is a solution which is orthogonalized to the core states on all other sites. J_{lm} and K_{lm} are defined as products of spherical harmonics and spherical Bessel and Neumann functions such that they are regular at the origin and at infinity, respectively, and both are regular at $\kappa = 0$.

We form a multicentered basis set of MTO's, i. e., the set of Bloch functions $\chi_{lm}^h(E, \kappa^2)$ for fixed parameters E and κ^2 , and apply the linear variational equation

$$\langle \chi_{lm}^h(E, \kappa^2) | H - E | \chi_{lm}^h(E, \kappa^2) \rangle = 0, \quad (1)$$

which is Eq. (15) in Ref. 8. All multicentered integrals are eliminated by using summation theorems for spherical Bessel and Neumann functions.

The low-energy valence bands as well as core states require a muffin-tin-orbital basis set with $\kappa^2 < 0$ (exponentially decaying states), whereas states near the Fermi surface (FS) require $\kappa^2 > 0$ (oscillating-plane-wave states). A very significant simplification in the LCMTO method is

achieved by enlarging the basis set to include both types of states. The secular equation is now in the LCAO form

$$\langle \chi_{l_1 m_1}^h(E_1, \kappa_1^2 < 0) + \chi_{l_2 m_2}^h(E_2, \kappa_2^2 > 0) | H - E | \chi_{l_1 m_1}^h(E_1, \kappa_1^2) + \chi_{l_2 m_2}^h(E_2, \kappa_2^2) \rangle = 0, \quad (2)$$

where E_1 is set equal to some average of the low-energy states and E_2 is set equal to some average of the states near the FS. Equation (2) is computationally simpler than Eq. (1) even with the larger basis set because the secular equation need not be calculated as a function of the energy E . This LCAO form is essential for complex crystals with many closely spaced energy bands.

Optimal values of the parameters are readily determined because the eigenvalues form broad minima as a function of $E_1, \kappa_1^2, E_2, \kappa_2^2$. These optimal values of the parameters are found to be independent of the particular \vec{k} -point symmetry if one desires 0.015 Ry or better agreement with the eigenvalues as calculated with Eq. (1).

The size of the basis set depends on the particular atoms involved but will not involve more than 18 MTO's per atom in the unit cell ($l = s, p, d$ MTO's for $\kappa^2 \geq 0$).

In the specific case of NiS an even smaller basis set is required. The sulfur $l = 3d$ MTO's can be omitted because the d states on a S atom are highly excited. The $l = 4p$ MTO's on the Ni were omitted after it was found that they were not necessary for convergence of the Ni $3d$ or $4s$ bands. However, we found that the Ni $3s$ core state must be included explicitly since the Ni core overlaps neighboring cores to an extent that makes orthogonalization to the Ni $3s$ impossible. The result is a 30×30 secular equation for NiS since there are four atoms per unit cell. The parameters are given in Table I for these 30 MTO's.

From experience with LCAO-type calculations, it would not appear necessary to include the $l = 0, 1$ $\kappa^2 > 0$ MTO's on the S atom. These states have no atomic analogy except being excited unbound states. However, these states contribute 0.03 Ry or more to some of the $3d$ bands and therefore must be included for accuracy of band energies.

III. POTENTIAL

Potentials are ordinarily constructed under the assumption that the atoms are at rest and at their equilibrium positions. However, for finite temperatures thermal lattice vibrations are excited and the nuclei undergo displacements from their equilibrium positions. A practical means of including an average electron-phonon coupling is to screen the $T = 0$ K potential by a Debye-Waller factor¹⁰ $e^{-W(G, T)}$. The Debye-Waller (DW) effect

TABLE I. Muffin-tin orbitals for NiS.

| l | S MTO's | | | | Ni MTO's | | |
|-------------------------|---------|------|------|------|----------|------|------|
| | 0 | 1 | 0 | 1 | 0 | 0 | 2 |
| $\kappa_l^2(\text{Ry})$ | -0.4 | -0.4 | -0.5 | 0.5 | -2.455 | 0.5 | 0.5 |
| $E_l(\text{Ry})$ | -1.8 | -1.1 | -0.7 | -0.7 | -8.00 | -0.7 | -0.7 |

has not previously been incorporated into first-principles band calculations because at least several-thousand reciprocal-lattice vectors are necessary to define the potential.

However, DW effects have been included in empirical pseudopotentials since only a few form factors $V(\vec{G})$ are necessary. For example, a DW factor was incorporated into the Cd pseudopotential to account for the anomalous temperature dependence of the Knight shift in Cd.¹² The DW effect also gives the correct temperature dependence of the optical-reflectivity peaks in Zn,¹³ PbTe,¹⁴ and GaAs.¹⁵

The crystal potential for NiS is constructed by overlapping atomic charge densities¹⁶ of Ni ($3d^8 4s^1$) and S ($3p^4 3s^2$). The potential is expanded in spherical harmonics $[\sum V_l^m(r) Y_{lm}(r)]$ within the atomic Wigner-Seitz cell. In order to reduce all integrals to radial integrals, the Wigner-Seitz cell potential $[\sum Y_{lm}(r) V_l^m(r)]$ is again expanded in spherical harmonics $[\sum \tilde{V}_l(r) Y_{lm}(r)]$ so that the potential is defined by spherical harmonics out to the farthest corner radius of the atomic WS cell. A particular $\tilde{V}_l(r) = \sum_{i,j} f_{i,j} V_{i,j}(r)$, where $f_{i,j} = \int_{\Omega_{\text{WS}}} Y_{i,j}^* Y_{i,j} d\Omega_{\text{WS}}$. The expansion in angular momentum was truncated at $l=8$ and $l'=8$. Potentials were constructed for lattice parameters corresponding to the low-temperature and high-temperature phases.

To include the DW screening $e^{-BG^2/16r^2}$, we Fourier analyze the high-temperature potential

$$\sum \tilde{V}_l(r) Y_{lm}(\vec{r}) = \sum V(\vec{G}) e^{i\vec{G}\cdot\vec{r}},$$

and then reconstruct the DW potential

$$\sum V(\vec{G}) e^{-BG^2/16r^2} e^{i\vec{G}\cdot\vec{r}} = \sum \tilde{V}_l(r) Y_{lm}(r).$$

$B=0.20 \text{ \AA}^2$ was taken from an x-ray structure determination on NiS by McWhan *et al.*⁷ The core part of the potential was replaced by the smooth function $(\sin\beta r)/\beta r$ so that 10 000 \vec{G} 's were adequate to expand the potential.

IV. ENERGY BANDS

The energy bands of NiS in its "normal d -band metal" t state are shown in Fig. 1 and the corresponding Brillouin zone in Fig. 2. The Ni $4s$ level lies well above the top of the d band at -0.25 Ry and is not shown. The S $3s$ bands are at about -1.7 Ry . The S p shell extends from -1.15 to -0.74 Ry so that it overlaps the d bands of Ni at the Γ point.

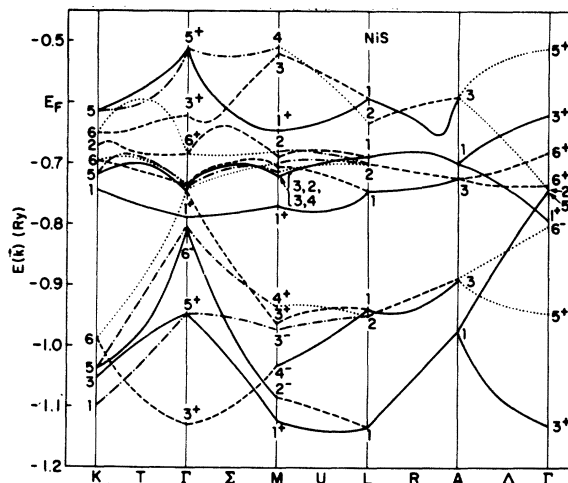


FIG. 1. Band structure of NiS in high-temperature metal state. For each symmetry line in the Brillouin zone, energy bands belonging to the same group symmetry are represented by lines of characters (dots, dashes, ...).

An understanding of the d bands requires examination of the NiAs structure. The most important aspect is that octahedra of sulfurs surrounding the metal atom are stacked to form metal-atom chains along the c axis. Consequently, the Z^2 orbital of the metal atom overlaps the Z^2 orbital of the adjacent metal on the chain. Since there are two Ni's per cell, bonding and antibonding combinations of the Z^2 orbitals occur at the Γ point. On the Brillouin-zone face ALH , the bonding and antibonding Z^2 states are degenerate. Thus, the Z^2 orbitals form a band, the width of which indicates the overlap or interaction strength between metal atoms. In NiS these Z^2 orbitals form a 0.16-Ry

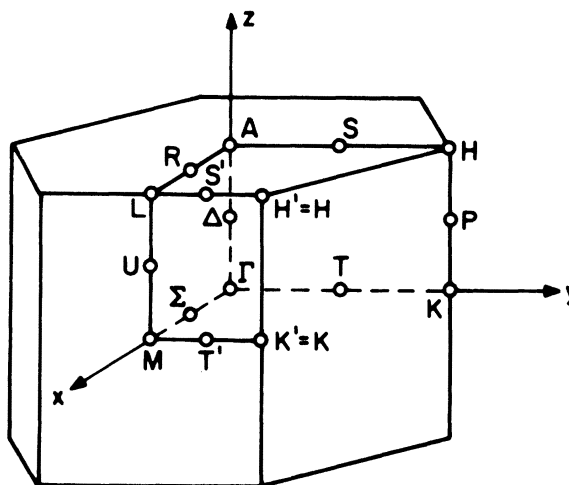


FIG. 2. Brillouin zone for the hexagonal space group D_{6h}^4 .

wide band since $\Gamma_1^+(Z_1^2 + Z_2^2) = -0.781$ Ry and $\Gamma_3^+(Z_1^2 - Z_2^2) = -0.621$ Ry. This treatment shows that the antibonding portion of the Z^2 band is near the Fermi surface (E_F approximately placed at -0.62 Ry) and will play a key role in conduction. Consideration of only the octahedral point symmetry of the Ni as in White and Mott³ and Koehler⁴ leads to the erroneous conclusion that the Z^2 orbital is narrow, nonbonding, and below the Fermi surface.

The remaining d -orbital bands are more complex. Certain bonding and antibonding combinations of d orbitals overlap strongly with sulfur p orbitals to form wide bands, whereas other combinations interact only weakly with $S p$ states and form narrow bands. The wide or p - d bands are near the Fermi surface and partially filled. The narrow bands are about 0.05 Ry wide and centered at about -0.7 Ry. In Fig. 1 one can identify which bands hybridize with p bands since each symmetry is identified by a character such as dots, dashes, etc.

A comparison is made in Table II of the effects of the discontinuous lattice expansion and thermal vibrations on the bands at the Γ point. The lattice expansion makes little difference as the bands are practically the same for the low-temperature and high-temperature lattice parameters. The bands which have the DW factor incorporated are different in that the overlap of the $S p$ bands with the Ni d bands is increased. The width of the narrow bands is about 0.05 Ry in all three cases, but examination of the wave functions indicates that hybridization with the p states increases for the DW case.

V. MOTT-HUBBARD STATE

Formation of a Mott-Hubbard state depends on the relative sizes of the intra-atomic Coulomb interaction ω with the bandwidth $\Delta \sim 0.08$ Ry and $\omega \sim 0.15$ Ry. They predict ω to be about one-half the value in NiO, a result of their hypothesis that the $S p$ bands overlap the bottom of the d bands. They also expect ω and Δ to be sensitive to the lattice parameters so that "the lattice distortion in conjunction with a fortuitous position of the Ni d

bands relative to the p bands"⁴ drives the Mott-Hubbard transition.

Our energy-band calculations support White and Mott's⁴ hypothesis that the $S p$ bands partially overlap the d bands and that the narrow bands are fortuitously close to the Fermi surface. Our energy-band calculations do not support their conclusion that ω and Δ are sensitive to the lattice distortion and drive the transition. We find that the overlap of the d and p bands is at least an order of magnitude more sensitive to thermal lattice vibrations than to the discontinuous lattice expansion.

We suggest that direct overlap of the d and p bands and also hybridization of the narrow d bands with p states both increase with T causing ω and Δ to be sensitive to T . At some critical T or average electron-phonon coupling, the Mott-Hubbard transition can occur because of the fortuitous position and width of the d bands in NiS. The discontinuous lattice distortion is likely a result of the transition in that there is charge redistribution to form the $1.66\mu_B$ moments.

The sensitivity of the wide bands to the DW factor might indicate that self-consistency could shift the relative positions of the p and d bands. The simplified LCMTO technique is economical enough to go to self-consistency if in the future data such as photoemission are collected.

Our bands cannot be quantitatively compared with other experimental data such as resistivity, Seebeck, susceptibility, and Hall because of the complicated Fermi surface. Qualitative interpretation would be similar to that of White and Mott and will not be repeated here. The theoretical model of Koehler⁵ is similar to that of White and Mott⁴ except that Koehler suggests that the p bands extend to the Fermi surface. The wide p - d bands we calculate eliminate the necessity of p bands at the FS to explain resistivity, Hall, and Seebeck data.

Finally, we relate the NiS band picture to the neighboring transition-metal sulfides, FeS and CoS. The a and c parameters in \AA are FeS (3.45, 5.67), CoS (3.37, 5.16), and NiS (3.42, 5.30). FeS has a moment of $\sim 4\mu_B$ and CoS has a moment of $\sim 1\mu_B$.

TABLE II. Temperature effects at Γ point.

| Ref. | Γ_1^+ | Γ^+ | Γ_2^- | Γ_5^+ | Γ_6^+ | Γ_6^- |
|------|---------------|---------------|---------------|---------------|---------------|--------------|
| a | -0.790 -0.260 | -1.138 -0.622 | -0.745 -0.744 | -0.947 -0.513 | -0.735 -0.686 | -0.803 |
| b | -0.776 -0.268 | -1.142 -0.632 | -0.727 -0.747 | -0.884 -0.521 | -0.732 -0.688 | -0.765 |
| c | -0.782 -0.299 | -1.029 -0.625 | -0.748 -0.743 | -0.936 -0.515 | -0.733 -0.688 | -0.799 |

^aHigh-temperature lattice parameters ($c = 5.3155 \text{ \AA}$, $a = 3.4431 \text{ \AA}$).

^bHigh-temperature lattice parameters with DW.

^cLow-temperature lattice parameters ($c = 5.3822 \text{ \AA}$, $a = 3.4535 \text{ \AA}$).

The metal atoms should have similar sizes but the metal-metal distances $\frac{1}{2}c$ are quite different. FeS should have the narrowest bands because the metal-metal and metal-sulfur overlap is the smallest. Thus, FeS can have a $4\mu_B$ moment if the narrow d and $p-d$ bands split with the Z^2 bands providing the metal states. CoS has the shortest metal-metal and metal-sulfur distances and therefore the widest bands. It is not surprising that CoS has a

smaller moment than NiS.

A similar calculation incorporating a DW factor is planned for VO_2 which undergoes a metal-insulator transition.

ACKNOWLEDGMENT

I would like to thank Dr. H. S. Jarrett for many helpful suggestions and a critical reading of this manuscript.

*Contribution No. 2010.

¹J. T. Sparks and T. Komoto, *Phys. Lett. A* **25**, 398 (1967).

²N. F. Mott, *Philos. Mag.* **20**, 1 (1969).

³J. T. Sparks and T. Komoto, *J. Appl. Phys.* **34**, 1191 (1963).

⁴R. M. White and N. F. Mott, *Philos. Mag.* **24**, 845 (1971).

⁵R. F. Koehler, Technical Report No. KSJ-821, Solid State Electronics Laboratory, Stanford, Calif., March, 1972 (unpublished).

⁶J. Trahan, R. G. Goodrich, and S. F. Watkins, *Phys. Rev. B* **2**, 2859 (1970).

⁷D. B. McWhan, M. Marezio, J. P. Remeika, and P. D. Dernier, *Phys. Rev. B* **5**, 2552 (1972).

⁸O. K. Andersen and R. V. Kasowski, *Phys. Rev. B* **4**, 1064 (1971).

⁹R. V. Kasowski and O. K. Andersen, *Solid State Commun.* **11**, 799 (1972).

¹⁰S. C. Yu, thesis (Harvard University, 1964) (unpublished).

¹¹*Methods in Computational Physics*, edited by B. Adler *et al.* (Academic, New York, 1968), Vol. 8.

¹²R. V. Kasowski, *Phys. Rev.* **187**, 891 (1969).

¹³R. V. Kasowski, *Phys. Rev.* **187**, 885 (1969).

¹⁴C. Ketter, T. M. Hayes, and A. Bienenstock, *Phys. Rev. Lett.* **21**, 1676 (1968).

¹⁵J. P. Walter, R. R. L. Zucca, M. L. Cohen, and Y. R. Shen, *Phys. Rev. Lett.* **24**, 102 (1970).

¹⁶F. Herman and S. Skillman, *Atomic Structure Calculations* (Prentice-Hall, Englewood Cliffs, N.J., 1963).

Electric Field Gradient at Ta in Group-IVB Metals. I. α -Zirconium

E. N. Kaufmann

Bell Laboratories, 600 Mountain Avenue, Murray Hill, New Jersey 07974

(Received 7 February 1973)

The first part of a program to investigate the nuclear electric quadrupole interaction at Ta in the group-IVB transition metals is reported. We have found, for Ta in hcp α -zirconium at room temperature, an interaction frequency ν_Q (482-keV state in ^{181}Ta) = 312 ± 3 MHz using the time-differential perturbed-angular-correlation technique. This corresponds to an electric field gradient at Ta in α -Zr of $|eq| = (5.1 \pm 0.2) \times 10^{17}$ V/cm². The results indicate a substantial electronic contribution to the magnitude and temperature dependence of the field gradient.

I. INTRODUCTION

The electric field gradient eq at a nucleus in a noncubic metallic environment arises from several sources. The so-called lattice contribution eq_{latt} from the lattice of positively charged ion cores can be calculated by straightforward summation techniques,¹ given the symmetry and lattice constants of the metal. The lattice contribution is enhanced at the nuclear site by the familiar Sternheimer antishielding factor² $(1 - \gamma_\infty)$, which is associated with the quadrupolar distortion of the closed electronic shells of the ion containing the nucleus in question. Fairly reliable values of γ_∞ for many of the elements can be found in the literature.^{2,3} In most instances experimental values for eq differ markedly from $(1 - \gamma_\infty)eq_{\text{latt}}$ because of the contri-

bution to the field gradient from conduction and valence electrons outside closed shells.⁴ The electronic contribution eq_{el} can be subdivided into two terms corresponding to electrons inside, $eq_{\text{el}}^{\text{loc}}$, and outside, $eq_{\text{el}}^{\text{dist}}$, of the Wigner-Seitz cell of the ion containing the nucleus of interest.^{5,6} The net effect of the distant electrons is to renormalize the effective ionic charges centered on lattice sites and can therefore be accounted for in the lattice sum mentioned above. In the cases studied,^{5,6} the renormalization has been shown to amount to only a few percent.

The effect of the local electronic structure, on the other hand, appears to dominate all other contributions to the field gradient and is crucial in determining the sign as well as magnitude of the net gradient at the nucleus. Two approaches to